PHYSICAL REVIEW B VOLUME 16, NUMBER 1 1 JULY 1977

Critical phenomena and magnetic properties of an amorphous ferromagnet: Gadolinium-gold*

S. J. Poon and J. Durand†

W. M. Keck Laboratory of Engineering Materials, California Institute of Technology, Pasadena, California 91125

(Received 2 August 1976)

Magnetization was measured between 4.2 and 290°K in fields up to 70 kOe on liquid-quenched $Gd_{80}Au_{20}$ amorphous alloys. The Curie temperature and critical exponents β, γ, and δ are found to be 149.45 ± 0.2°K, 0.44 ± 0.02, 1.29 ± 0.05, and 3.96 ± 0.03, respectively. The data are fitted to an equation of state previously derived for a second-order phase transition in fluid systems. It is found that the magnetization exponent β of amorphous ferromagnets studied so far has a value ~ 0.4, slightly enhanced over those observed in corresponding crystalline elements, and the estimated specific-heat exponent α is negative. Both are in qualitative agreement with theories on the critical behavior of random systems. The effects of structural disorder on the magnetic properties studied are compared and discussed with recent theories on amorphous magnetism. A comparison of the magnetization data with Handrich's theory for amorphous ferromagnets suggests that in our amorphous alloys the average fluctuation in the exchange constant (J) can be an appreciable fraction of J itself. The effective magnetic moment in the paramagnetic state has a value of $(8.9 \pm 0.1)\mu_B$ per gadolinium atom. The saturation moment extrapolated to 0°K equals $(7.0 \pm 0.25)\mu_B$ per Gd atom. The low-temperature saturation magnetization follows the $T^{3/2}$ law from 0.13 T_c to 0.80 T_c. The mean exchange integrals J determined from the Rushbrooke-Wood formula and spin-wave theory are found to be 2.28 ± 0.15°K and 1.34 ± 0.08°K, respectively. The exchange constant of the Ruderman-Kittel-Kasuya-Yosida interaction as estimated from the de Gennes model ($J_{sf} \simeq 0.19$ eV) is not drastically reduced in this amorphous matrix. Finally, the Curie temperature of pure amorphous Gd is estimated and its value compared with those obtained from experimental extrapolation.

I. INTRODUCTION

Magnetism in structurally amorphous alloys has been the subject of considerable interest not only as a topic in solid state physics, but also because of its technological potential. Rare-earth-transition-metal binary alloys in the amorphous state have been prepared in bulk form by d.c. rapid sputtering and by coevaporation as thin films.[1-3] Amorphous rare-earth–noble-metal alloys have also been prepared by these techniques,[3-5] and by the method of liquid quenching.[6] The compositional ranges of the systems investigated with the exception of Gd-Ag alloys[4] are on the transition-metal side of the binary phase diagrams. Previous attention has been focused on compositions corresponding to some crystalline counterparts[1] (e.g., R-Fe_2, where R = Ho, Gd, Tb, and Y). Magnetization and Curie temperature measurements have been carried out to study the magnetic properties (e.g., magnetic moments, local anisotropy, and exchange interactions, etc.) of the alloys. A mean-field model of the magnetic properties of R-Fe_2 amorphous alloys has been developed[7,8] which incorporates a Fe spin whose dependence on parameters is derivable from Mössbauer spectra. The magnetic structures for both transition-metal and rare-earth moments have been studied by neutron scattering and Mössbauer-effect measurements.[9]

Besides these measurements, there was a basic problem of whether or not a second-order magnetic phase transition can exist in random systems. Theoretical investigations using renormalization-group analysis and cumulant expansion technique in the Ising spin models and isotropic Heisenberg spin models were made for these systems.[10-13] Criteria for observing a sharp transition in a random alloy were discussed. Meanwhile, magnetization and specific-heat measurements were carried out[14] on splat-cooled amorphous transition-metal alloys. For some of the systems studied, particularly the Co-P-B, Fe-P-C and Metglass 2826A alloys, the results indicated a sharp transition with well-defined critical exponents. The reduced magnetization and field follow an equation of state derived for second-order phase transition in fluid systems,[15] with the critical exponents satisfying an equality relation. Previous experiments have been performed to investigate the critical behavior of ferromagnets in the crystalline state.[16-19] Most of the materials studied have critical exponents quite close to the theoretical values derived from the Heisenberg model. A similar trend was also observed in amorphous ferromagnets[14] near the Curie temperature, indicating the dominance of short-range forces.

In amorphous transition-metal alloys where the d-d overlaps play a significant role on their magnetic states, the amorphous ferromagnetism is discussed in terms of a distribution of the Heisenberg exchange interaction.[20-22] There exist other microscopic theories[23-27] which predict the magnetic properties of disordered alloys using the site diluted or bond random models. In the rare-earth–

transition-metal alloys (such as $HoFe_2$ and $TbFe_2$), it is suggested[28] that the Ruderman-Kittel-Kasuya-Yosida (RKKY) exchange interaction[29] between the magnetic atoms is constant and the amorphous nature of the alloy is manifested in a random distribution of local anisotropy field. However, the situation might be different in our amorphous Gd-Au alloys where Gd is an S-state ion. The anisotropy field effect is expected to be small and one can focus on the other effects of amorphousness on the magnetic properties.

We report here the results of magnetization measurements for bulk amorphous $Gd_{80}Au_{20}$ alloys obtained by liquid quenching. Gold is chosen as the glass former, both for metallurgical reasons and for the fact that it contains no unfilled d and f shells. The purpose of this paper is twofold. First, a detail study is made on the critical behavior of amorphous $Gd_{80}Au_{20}$ alloys around its Curie temperature. We determine the spontaneous magnetization and initial susceptibility values in the critical region. This allows determinations of the critical exponents and T_c. Magnetization results of single-crystal[19,30,31] Gd were found to depend strongly on the crystal axis along which the field was applied. Measurements on amorphous Gd are expected to yield an averaged result of some corresponding crystalline values. Possible asymptotic equations of state are to be investigated following the work of Kouvel and Comly.[32] An attempt is made to compare the results of different amorphous alloys with existing theories on the critical behavior of disordered systems. The roles played by different forces in the vicinity of Curie transition are also considered. Second, we study the effect of structural randomness on the magnetic properties [effective moment μ_{eff}, saturation moment μ_{Gd}, T_c, spontaneous magnetization $M_s(T)$, and saturation magnetization $M(\infty, T)$] of $Gd_{80}Au_{20}$. Comparison of the present results with those of crystalline compounds and solid solutions is made. These results are extrapolated to the case of pure amorphous Gd and compared with theoretical predictions whenever possible.

The format of this paper is as follows. In Sec. II, experimental procedures and results are presented. Section III consists of three subsections from A to C. Section III A describes the processing of raw data to obtain final data for analysis. In Sec. III B 1, critical behavior around T_c is investigated using data from detail magnetization measurements up to ~40 kOe for every degree in the temperature range $|T - T_c| \leq 10$ °K. The critical exponents are discussed in terms of models and local interactions. Section III B 2 presents an equation of state graphically. The parameters involved come from the scaling law hypothesis. Asymptotic equations of state very close to T_c are also obtained and discussed. Section III C gives the values of μ_{eff}, μ_{Gd}, $M_s(T)$, and $M(\infty, T)$. These values are compared and discussed with those of crystalline systems. The values of the mean exchange integrals are obtained from the spin-wave theory[33] and the Rushbrooke-Wood formula.[34] The effects of structural randomness on the magnetic properties are discussed. The last section is the summary and conclusion.

II. EXPERIMENTAL PROCEDURES AND RESULTS

The $Gd_{80}Au_{20}$ alloys were prepared by induction melting of the appropriate constituents on a silver boat under an argon atmosphere. Samples were then quenched from the liquid state using the "piston and anvil" technique described in Ref. 35. The cooling rate is estimated to be of the order 10^6 °C/sec. Samples prepared by this technique were in the form of foils with surface area of ~2×2 cm and thickness of about 40 μm. The structure of each sample was checked by x-ray scanning with a Norelco diffractometer. Only samples containing a single amorphous phase were retained for detailed experimental studies. The x-ray diffraction patterns ($CuK\alpha$) of these samples were characterized by a broad maximum centered at 32.8° with a full width at half maximum at 4.6°. According to the Sherrer formula, this corresponds to an effective microcrystal size of ~17 Å, which is typical of a glassy metal.[36] It should be added that by analyzing our magnetization data we found a small amount of crystallization in the samples (≃2% of a sample) which cannot be detected by the rapid x-ray scanning technique. No significant annealing effect is observed for the amorphous phase at room temperature during periods of several weeks. Spontaneous crystallization is observed at temperatures of about 200–250 °C.

The Curie temperature T_c was observed using a standard ac inductance bridge technique. The T_c estimated from the inflection point of the signal intensity was found to be ~149 °K. Magnetization measurements as functions of magnetic field and temperature were carried out by using the Faraday method with an Oxford Instruments Magnetometer described elsewhere.[37] Samples used in the $M(H, T)$ measurements were in the form of disks (3 mm in diameter) punched from foils. The thermal output control for the temperature has an accuracy of 0.05 °K. Measurements for $M(H)$ were made approximately every 20 °K from 4 to 290 °K except near T_c, and for fields up to 70 kOe. Near T_c (≃149 °K), measurements were made every 1 °K in the temperature range 136–160 °K, and for fields up to 40 kOe.

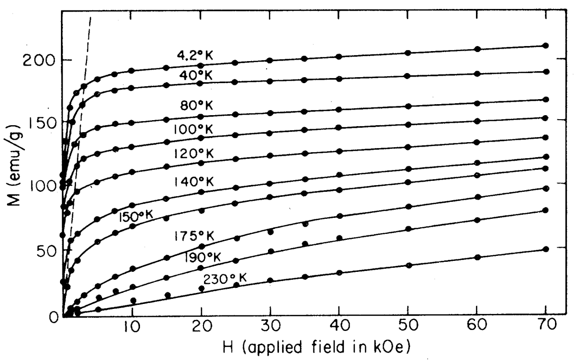

FIG. 1. Magnetization vs applied field up to 70 kOe for different temperatures ($4.2° \leq T \leq 230$ °K). The dashed line indicates the demagnetizing effect correction.

Figure 1 illustrates representative high field isotherms $M(H)$. In Fig. 2, $M(T)$ for constant magnetic fields were plotted. It is noticed that the small kink or inflection point expected at T_c is not detectable for fields higher than 2 kOe. For small H, the Curie temperature is given by the inflection point, because for T just greater than T_c, M is dominated by a large initial susceptibility χ_0, which has a hyperbolic dependence on temperature. For large H, the disappearance of the inflection point at T_c is attributed to the magnetic inhomogeneities in the vicinity of T_c.[38]

III. ANALYSIS AND DISCUSSION

A. Processing of data

In order to discuss the results, it is necessary to know the $M(H, T)$ values of the magnetic amorphous phase and the effective applied field H corrected from the demagnetizing field. Thus corrections must be made for any possible magnetic precipitates from the matrix and demagnetization effects. The presence of small amounts of crystalline inclusions is rather common in splat-cooled samples.[39] This amount of ferromagnetic precipitates varies between the center and the foil edges, but this quantity was subtracted from the total magnetization, then the temperature and field dependence of the remaining contributions attributed to the amporphous phase was found to be the same for a given foil. The existence of crystalline gadolinium precipitates in the matrix is evidenced by noticing two facts. For $T \gtrsim 190$ °K (far from T_c), $M(H)$ still exhibits appreciable curvature at fields up to ~5 kOe. Above T_c, remanent magnetization is observed which diminishes with increasing temperature and vanishes at ~290 °K. A general feature of these curves is observed. There is an intermediate field region (5–20 kOe) where linearity can be defined. Above 20 kOe, the $M(H)$ curves show small curvatures (see Fig. 1). We reproduce representative data in Fig. 3 for $T \gtrsim 190$°K and $H \lesssim 20$ kOe. The field dependence of the high-temperature isotherms is analyzed as follows. The magnetization of Gd precipitates saturates around 5 kOe. The linear region at $5 \lesssim H \lesssim 20$ kOe gives the initial susceptibility χ_0 of the amorphous phase at $T \gtrsim 190$ °K. The extrapolation of the linear portion to $H=0$ gives the saturation magnetization M'_∞ for the precipitates. A systematic decrease in M'_∞ at increasing temperature is then obvious. The small curvatures observed for $M(H)$ above 20 kOe at $T \gtrsim 190$ °K suggest the presence of short-range magnetic ordering above the Curie temperature as will be discussed later. To verify that the M'_∞ values are in fact due to ferromagnetic contributions from gadolinium precipitates in the amorphous matrix, we compare in Fig. 4 the Debye-Weiss curve for $S=\frac{7}{2}$ and $T_c \approx 293$ °K,[30] with the M'_∞ values for $T > 190$ °K obtained from Fig. 3. For pure crystalline Gd,[40] similar agreement was reported for $0.9 \gtrsim T/T_c \gtrsim 0.6$. At low temperatures, maximum de-

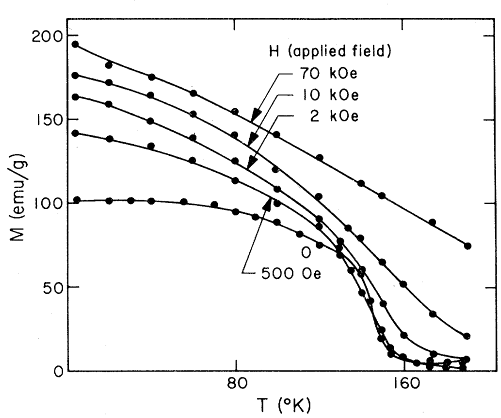

FIG. 2. Magnetization vs temperature for different applied fields ($0 \leq H \leq 70$ kOe).

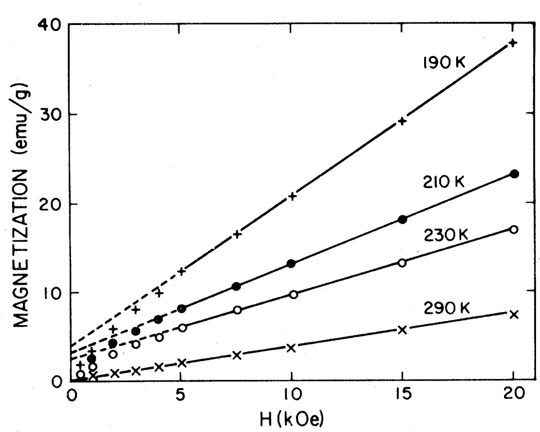

FIG. 3. Magnetization vs applied field (up to 20 kOe) for temperatures $\gtrsim 190$ °K.

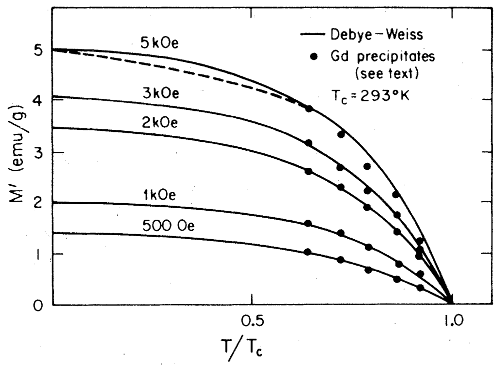

FIG. 4. Magnetization M' for Gd precipitates at different fields vs reduced temperature T/T_c with $T_c = 293$ °K. The saturated magnetization obtained at 5 kOe is fitted to a Debye-Weiss curve with $S=\frac{7}{2}$.

viations of ~ 4% due to spin-wave excitations were observed,[40] as indicated by the dashed curve. At 0 °K the contributions from crystalline inclusions represent only 2.5% of the total saturation magnetization for our sample. But in the critical region for the amorphous phase (around 150 °K) and for the low-field data ($H<5$ kOe), both crystalline and amorphous contributions have the same order of magnitude. These difficulties were apparently overlooked in previous studies[14] on the critical behavior in amorphous ferromagnets. We determine in a consistent way the amorphous contribution and the magnetization due to Gd precipitates by exploiting our data graphically. In Fig. 3, we obtain the isotherms at $T>190$ °K for the precipitates by plotting $M'(H)=M(H)-\chi_0 H$, where χ_0 is determined from the linear part of $M(H)$ ($5\le H\le 20$ kOe). It is observed that the $M'(H,T)$ data at fields below 5 kOe follow the smooth curves as shown in Fig. 4. The shape of these curves resembles somewhat the one at 5 kOe which is fitted to a Brillouin function ($S=\frac{7}{2}$; $T_c=293$ °K). The monotonic behavior of $M'(H,T)$ allows us to determine the values of the Gd precipitates magnetization for $H<5$ kOe and $140\le T\le 160$ °K. The uncertainty involved in this process is estimated to be ~5%. It should also be mentioned that the uncertainty on the raw data is ~0.5%.

The demagnetizing constant is determined from averaging the initial slopes of the corrected $M(H)$ curves below T_c.[31] The average value of the initial slopes over the temperature range $4<T<140$ °K is approximately 70 emu/g kOe. This correction method simply assumes that $\chi_0^{-1}=0$ below T_c. At low fields, the samples tend to deflect slightly from the center of the sample tube to a position where the field direction is not known.[37] Thus the geometric interpretation of this demagnetizing constant is not obvious and should not be taken seriously. It is just an averaged result. The value 70 emu/g kOe for the demagnetizing constant can be verified consistently by noticing that the $M(H)$ curves around T_c (determined later) should intercept the demagnetizing line only at the origin as shown in Fig. 1. Corrections for the demagnetizing factor and for the crystalline inclusions are taken into account in the analysis presented in Sec. III B.

B. Critical behavior and the magnetic equation of state

1. Critical exponents

The second-order phase transition around the Curie point is characterized by a set of critical exponents and a magnetic equation of state. Relations between the exponents are obtained by the scaling hypothesis approach developed by several authors.[15,41-43] The results of the static scaling approach indicate that the exponents should be adequately described by two parameters. Here we will discuss the three exponents β, γ, and δ for the present system. The exponents β and γ are those describing the temperature dependence of the spontaneous magnetization ($H=0$) just below T_c

$$M_s \sim |T-T_c|^\beta , \qquad (1)$$

and that of the initial susceptibility just above T_c

$$\chi_0 \sim |T-T_c|^{-\gamma} . \qquad (2)$$

The exponent δ describes a relation between M and H at T_c

$$M \sim H^{1/\delta} . \qquad (3)$$

The scaling law implies

$$\gamma = \beta(\delta-1) , \qquad (4)$$

and a simple form of the magnetic equation of state in the critical region given by

$$h/m = f_\pm(m) , \qquad (5)$$

where the plus and minus signs denote temperatures above and below T_c, respectively. The normalized quantities are $m=M/|1-T/T_c|^\beta$ and $h=H/|1-T/T_c|^{\beta\delta}$. First, we present and justify the graphical method we used for the determination of T_c and of the critical exponents. Then, we give the results of our analysis with an estimate of the uncertainties. Finally, we compare our results with theoretical predictions.

a. Method. The exponents of the amorphous $Gd_{80}Au_{20}$ alloys will be determined by the graphical method using Eqs. (1)–(3). A conventional technique developed by Arrott[44] and Kouvel[45] was to plot the data at various temperatures as M^2 vs H/M. This convenient method was based on the molecular-field theory. It can be understood by expanding the self-consistent mean-field relation $M_\infty = M$

$B_s[\mu(H+\lambda M)/kT]$ for small H around T_c, where B_s is the Brillouin function for spin quantum number S, μ is the magnetic moment per atom, and λ is the exchange coupling constant. It can be shown that $\beta = \frac{1}{2}$, $\gamma = 1$, and $\delta = 3$ using this approach. The intercepts along the M^2 axis (i.e., $H/M = 0$) and H/M axis (i.e., $M^2 = 0$) give the square of the spontaneous magnetization M_s^2 and inverse initial susceptibility χ_0^{-1}, respectively. If $\delta = 3$, the initial slopes of M^2 vs H/M should be almost equal by considering the equation of state around T_c, and the intercepts can be determined conveniently. Unfortunately, it has been observed that δ is closer to four than three, which gives large gradients

$$\frac{dM^2}{d(H/M)} \sim |T - T_c|^{\beta(3-\delta)}$$

near T_c. The fact that the isotherms $M^2(H/M)$ and the M^2 axis are almost parallel introduces difficulties in determining M^2 accurately. In fact, experimental results in the literature[16] indicate that it is easier to obtain $(H/M)_{M=0}$ than M_s^2 because of the large gradients near T_c. Following the work of Arrott and Noakes,[17] Mizoguchi *et al.*[14] obtained M_s and χ_0 by plotting $M^{2.5}$ vs $(H/M)^{0.75}$. However, there is no *a priori* reason to plot $M^{1/\beta}$ vs $(H/M)^{1/\gamma}$, since the exponents are not yet determined. Even if β and γ are known, it is not clear that this plot is physically meaningful or that it does give the correct values of M_s and χ_0^{-1}. In fact, the equation of state proposed in Ref. 17 is in conflict with the results of Kouvel *et al.*[32] at low fields. We proceed in a slightly different fashion. We first determine $\chi_0^{-1}(T)$ using the conventional M^2-vs-H/M plot. Equation (2) tells us that a plot of the inverse of $d\log_{10}\chi_0^{-1}(T)/dT$ vs T should give a straight line near T_c. The reciprocal gradient of the straight line and its intercept with the T axis should give the exponent γ and T_c, respectively. Knowing T_c, we plot $\log_{10}M$ vs $\log_{10}H$ from Eq. (3) to obtain δ. These values of γ and T_c can be checked consistently when we determine β later. Then we plot M^p vs H/M to determine M_s^p, where p is a convenient integer slightly larger than $\delta - 1$. It is hoped that the gradients

$$\frac{dM^p}{d(H/M)} \sim |T - T_c|^{\beta(p+1-\delta)}$$

near T_c are finite and almost equal to the value of $dM^{\delta-1}/d(H/M)$ at T_c. Using Eq. (1), a plot of the inverse of $d\log_{10}M_s/dT$ vs T should give a straight line with gradient equal to β^{-1} and intercept at T_c along the T axis.

b. Analysis. In Fig. 5, M^2 is plotted against H/M for $T > T_c$. The intercepts at $M = 0$ give the reciprocal initial susceptibility χ_0^{-1}. When we plot χ_0^{-1} vs T, the uncertainty $\delta M'$ [±5% of crystalline contributions to $M(H)$] mentioned in Sec. III A, must be taken into account. By doing so, the points $(M^2, H/M)$ are shifted to $[M^2(1+2\,\delta M'/M),\ (H/M)(1-\delta M'/M)]$. An order of magnitude of $\delta\chi_0^{-1}$ can be estimated assuming that the portions of $M^2(H/M)$ are rather linear below 500 Oe: for T between 150 and 160 °K, $\delta M' = \pm 0.04$ emu/g at 500 Oe (Fig. 4), and $M \simeq 2$ emu/g; thus giving $\delta\chi_0^{-1} \simeq \mp 0.02(H/M)500$ Oe. To determine the exponent γ we rewrite $1/(d/dT)\log_{10}\chi_0^{-1}$ as $1/\chi_0(d\chi_0^{-1}/dT)$. The values of both χ_0^{-1} and $d\chi_0^{-1}/dT$ are determined from the $\chi_0^{-1}(T)$ curve. Such experimental details have been discussed fully in Ref. 18 and will not be repeated here. However, two corrections must be made in differentiating χ_0^{-1}. The first concerns drawing a smooth curve through the χ_0^{-1} data points. Small variations are possible thus giving uncertainty bounds on $d\chi_0^{-1}/dT$. Second, the temperature T at which the local derivative $d\chi_0^{-1}/dT$ is defined is uncertain to within ±0.05 °K. Finally, an intrinsic uncertainty of ±0.05 °K associated with the performance of the thermal output must also be considered. All these when taken together give two-dimensional uncertainty bars in the plot of $1/(d/dT)\log_{10}\chi_0^{-1}$ vs T. Such plot is shown in Fig. 6. The size of the close-circled points can

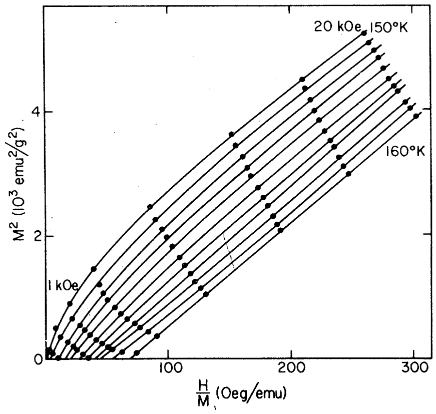

FIG. 5. M^2 vs H/M for every °K from 150 to 160 °K.

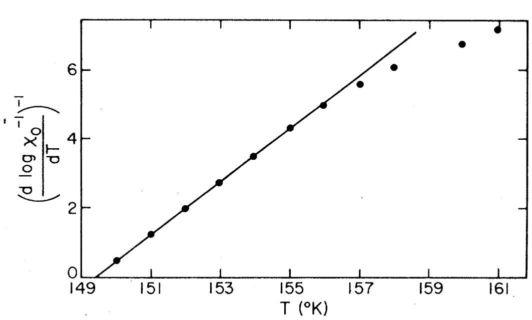

FIG. 6. Inverse of $d\log_{10}\chi_0^{-1}/dT$ vs temperature gives the critical exponent γ and Curie temperature T_c according to text.

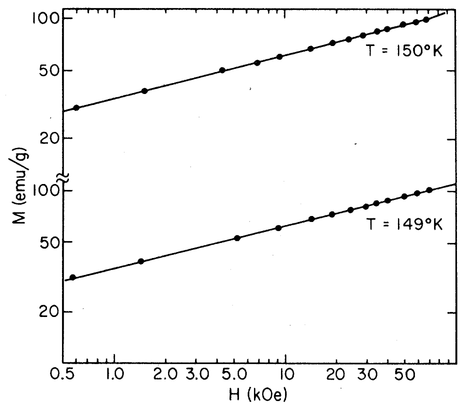

FIG. 7. $\mathrm{Log}_{10}M$ vs $\log_{10}H$ for 149 and 150 °K.

already account for the experimental uncertainties. The straight line obtained from a least-square fit through the centers of the circles gives values of $\gamma = 1.29$ and $T_c = 149.45$ °K. Then the least-square fits through the edges of the circles to yield the maximum uncertainties give $\gamma = 1.29 \pm 0.05$ and $T_c = 149.45 \pm 0.2$ °K. It should be mentioned that these results have been checked by an iterating scheme together with the determinations of β and δ.

In Fig. 7, the values of $\log_{10}M$ vs $\log_{10}H$ are presented for the two temperatures 149 and 150 °K for fields from 500 Oe to 70 kOe. The reciprocal gradients so obtained represent the values of δ for the two temperatures. They are found equal to 3.98 and 3.94, respectively. Since these two values are almost equal for temperatures ±0.5 °K from T_c, it might not be meaningful to determine δ by repeating a measurement of $M(H)$ at 149.45 °K. Perhaps it is more relevant to compare these values of δ with the one obtained from Eq. (4) knowing β and γ. The uncertainty in δ is found to be small compared with that in the γ value. This can be understood roughly as follows: the fractional uncertainty in δ is estimated from

$$1 - \log_{10}M/\log_{10}(M + \delta M') \approx (\delta M'/M)/\log_{10}M,$$

$$\delta M' \simeq 0.2 \text{ emu/g}, \quad M \simeq 50 \text{ emu/g}$$

for $H > 5$ kOe (Figs. 4 and 7); thus giving a small uncertainty of 0.001δ. Likewise, the effect due to fluctuations in the applied field associated with the performance of the apparatus can be estimated at 500 Oe and higher fields; the fluctuation $\delta H/H \simeq 0.003$ adds another error of 0.001δ. Errors in the graphical determination of δ should also be included.

Knowing δ, the aforementioned parameter $p(\approx\delta - 1)$ is taken to be 3. In Fig. 8, M^3 is plotted versus H/M. It is seen that the lines are almost parallel at small H/M for temperatures ranging from 149 to 136 °K. The initial gradients make it easier

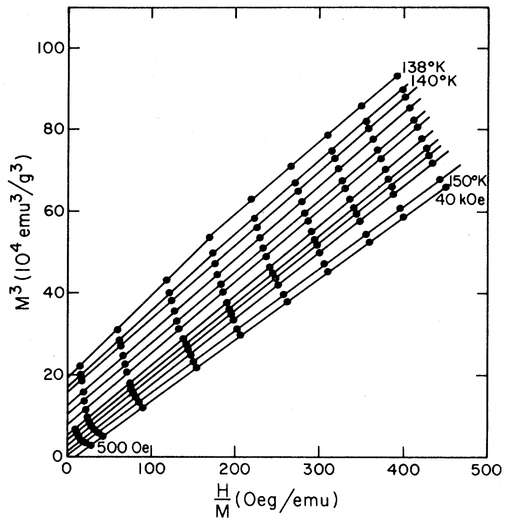

FIG. 8. M^3vs H/M for every °K from 140 to 150 °K. The curve for 138 °K is also included.

to determine M_s^3 and thus M_s. We can correct the crystalline contribution to M_s in a similar fashion as we did for χ_0^{-1}: Assuming that the curves are rather linear below 500 Oe, $M \gtrsim 10$ emu/g and $\delta M' \lesssim 0.05$ emu/g at 0–500 Oe for $T \lesssim 148$ °K, the uncertainties δM_s when propagated to $H/M = 0$ are bounded by ±0.005 times the magnetizations at 500 Oe, since $\delta M'$ is smaller at decreasing H/M. Again, we rewrite $1/(d/dT)\log_{10}M_s$ as $M_s/(dM_s/dT)$ and obtain the quantities M_s and dM_s/dT from the M_s-vs-T plot. This is proceeded in a similar way as discussed beforehand. With the uncertainties both in M_s and T manifested by the closed-circle points, the mean straight line in Fig. 9 determines $\beta = 0.44$ and $T_c = 149.45$ °K after an iterating process. Corrected values from other straight lines give $\beta = 0.44 \pm 0.02$ and $T_c = 149.45 \pm 0.2$ °K. Substituting $\gamma = 1.29 \pm 0.05$ and $\beta = 0.44 \pm 0.02$ in Eq. (4) implies $\delta = 3.93 \pm 0.26$ within the range of the values determined earlier for $T = 149$ and 150 °K. How-

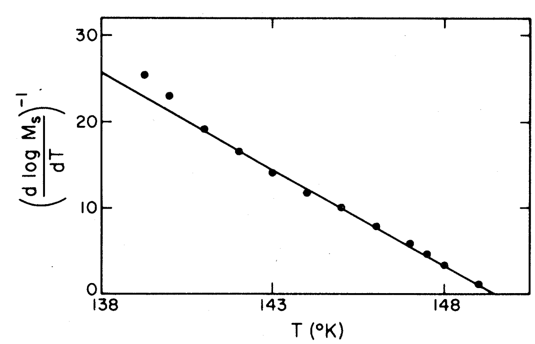

FIG. 9. Inverse of $d\log_{10}M_s/dT$ vs temperature gives the critical exponent β and Curie temperature according to text.

ever, such a large uncertainty is unlikely in view of the former determination of δ (uncertainty of 0.002δ). We would rather take a value of δ extrapolated to 149.5 °K from the two values determined beforehand. Thus, without loss of accuracy, we determine $\delta = 3.96 \pm 0.03$ taking also into account all the experimental and graphical uncertainties.

c. Discussion. First, we comment on our critical exponent values and on the experimental temperature range for the scaling behavior in terms of Heisenberg model and mean-field theory. Then we discuss the trend of enhanced values for β as observed in amorphous ferromagnets. Finally we compare our calculated values for the critical exponent α with model predictions for amorphous magnetism.

Model calculations of the critical exponents have been made for the Ising and Heisenberg models for several dimensionalities d and spins S. It is argued that the applicability of these results depend both on the dimensionality d and the nature of the interactions which determines a parameter d^*; whether they are long-range, short-range, or uniaxial forces. Derivations of these relations are reviewed by Kadanoff[15] using the renormalization-group theory. In particular, for short-range interactions with $d^* = 4 > d$, one expects to observe nonclassical exponents. A summary of theoretical and experimental amorphous results is presented in Table I. It can be seen that the experimental values follow fairly well the Heisenberg predictions, indicating the dominance of short-range forces. Similar trend has been observed in crystalline ferromagnets. We include in Table I the Co, Fe, and Gd results for comparison. According to the estimate of Kadanoff *et al.*,[46] long-range forces (e.g., dipolar forces) should affect the critical fluctuations of the magnetization within the temperature range defined by

$$1 - T/T_c \approx (\mu M_\infty / kT_c)^{1/\beta(\delta-1)} \equiv t_c ,$$

where $\mu = g\mu_B S$ is the moment per spin and M_∞ the saturation magnetization. For the present Gd-Au alloys, $S = \frac{7}{2}$, $M_\infty \approx 1800$ Oe, and $T_c \approx 150$ °K one obtains, taking $\beta(\delta - 1) \approx 1.29$, a value $t_c \approx 0.015$. Experimentally, we determine the critical exponents in the regions $\epsilon = |1 - T/T_c| < 0.06$ for $T < T_c$; and $|1 - T/T_c| < 0.04$ for $T > T_c$. Similar or more extended critical regions of β have also been observed in other amorphous ferromagnets.[14] The fact that our experimental values for ϵ are larger than the temperature range for long-range interactions as defined by Kadanoff may explain that the critical exponents for amorphous $Gd_{80}Au_{20}$ do not depart too strongly from the Heisenberg predictions. Nevertheless, contrarily to the Metglass 2826A case,[14] the fact that $\epsilon \sim 4\, t_c$ does not allow us to rule out any long-range force influence in our

TABLE I. Experimental values of critical exponents γ, β, and δ for amorphous alloys and crystalline elements. The specific-heat exponents α listed in this table are evaluated from γ and β. Theoretical three-dimensional Heisenberg values are also included.

	γ	β	δ	α
Three-dimensional Heisenberg[a]	$\frac{4}{3}$	0.33 – 0.37	4.2	
Cobalt[b]	1.23 ± 0.05	$\sim 0.36 \pm 0.08$		0.05 ± 0.21
Gadolinium (Ref. 19)	1.19	0.38	3.61	0.06
Iron[c]	1.30 ± 0.06	0.37 ± 0.03		-0.04 ± 0.12
Iron[d]	1.33	0.389	4.35	-0.10
Nickel (Ref. 32)	1.34	0.378	4.58	-0.10
Amorphous $Co_{70}P_{20}B_{10}$[e]	1.34 ± 0.025	0.40 ± 0.01	4.39 ± 0.05	-0.14 ± 0.05
Amorphous $Fe_{80}P_{13}C_7$[f]	1.30 ± 0.05	0.38 ± 0.02	4.47 ± 0.05	-0.06 ± 0.09
Metglass 2826A[g] ($Fe_{32}Ni_{36}Cr_{14}P_{12}B_6$)	1.67 ± 0.08	0.41 ± 0.02	5.07 ± 0.20	-0.49 ± 0.12
Amorphous $Gd_{80}Au_{20}$[h]	1.29 ± 0.05	0.44 ± 0.02	3.96 ± 0.03	-0.17 ± 0.09

[a] S. Milosevic and H. E. Stanley, Phys. Rev. B 6, 986 (1972); 5, 2536 (1972); K. Binder and K. Müller-Krumbhaar, *ibid.* 7, 3297 (1973).
[b] C. J. Glinka and V. J. Minkiewicz, AIP Conf. Proc. 24, 283 (1974), and references cited therein. In the absence of detailed magnetization studies in the critical region, the exponent β is estimated from the scaling theory relation $d\nu = \gamma + 2\beta$.
[c] M. F. Collins, V. J. Minkiewicz, R. Nathans, L. Passell, and G. Shirane, Phys. Rev. 179, 417 (1969).
[d] S. Arajs, B. L. Tehan, E. E. Anderson, and A. A. Stelmach, Int. J. Magn. 1, 41 (1970).
[e] T. Mizoguchi and K. Yamauchi, J. Phys. (Paris) 35, C4–287 (1974).
[f] K. Yamada *et al.*, Solid State Commun. 16, 1335 (1975).
[g] E. Figueroa *et al.*, Solid State Commun. 20, 961 (1976).
[h] Present work.

case. *A priori*, long-range interactions are expected to be significantly reduced in amorphous materials with a very-short mean free path.[47] Experimentally, these interactions (dipolar, RKKY) are still evidenced in amorphous rare-earth alloys[48] and one does not know yet how much they are reduced as compared with those in the crystalline counterpart.

As shown in Table I, a trend of enhanced values of β ($\beta \geq 0.40$) is observed in amorphous alloys compared with elemental crystals. Since all the amorphous alloys studied so far contain at least one nonmagnetic component (20 at.% and more), this trend may be tentatively explained in terms of a dilution model. Müller-Krumbhaar[13] has investigated the critical behavior of magnetization in a homogeneous Heisenberg spins system with one missing cluster of $\sim 2^3$ spins. He found that the local value β_l close to the missing cluster changes from 0.33–0.41 near $|1 - T/T_c| \simeq 0.05$. This can be understood in simple physical terms: β_l will be influenced by "surface effects" (which enhances β_l) when the correlation length ξ is smaller than the length of the defect (say twice the lattice constant $2a$); this sets the changeover temperature t_c through $\xi_0 |t_c|^{-\nu} = \xi < 2a$, where ν is the critical exponent relating ξ to $|1 - T/T_c|$, thus giving $|t_c| > (\xi_0/2a)^{1/\nu}$. As the concentration of defects or clusters of missing spins increases, one would expect the bulk value of β to increase as well. The application of this model to highly inhomogeneous systems awaits further theoretical investigations along this line. So far, the small enhancements of β in amorphous alloys have been a general trend which might be related to the weakening of short-range interactions in a lattice randomly diluted with numerous "missing spins." This weakening is also manifested in the reduction in J, the exchange constant between spins, as will be discussed in a later section.

The critical behavior of disordered systems has been studied by several authors.[10-13] In these theoretical models, randomness both in bond defects and in the exchange constant J (the so-called magnetic glass model) is considered. It is shown that in a disordered n-component spin system with $1 < n < 4$, a sharp transition is only possible if its specific-heat exponent α is nonpositive. Simple physical arguments can be used to support the formal calculations of Refs. 10–13. The basic concept is that in order to have a sharp transition with respect to fluctuations, the correlation length ξ defined at some temperature close to the Curie temperature cannot be larger than that corresponding to the half width of some T_c distribution due to fluctuations. One then obtains the condition $\frac{1}{2}\alpha = 1 - \frac{1}{2}d\nu \leq 0$, where ν is the correlation length exponent. In a multicomponent amorphous alloy, both compositional disorder and structural disorder are present. The condition for a sharp transition should apply equally well to both disordered crystalline and amorphous systems, since the theoretical models yield the same requirement on α for randomness in both bond defects and exchange constants. However, it would still be interesting to study the critical behavior in materials with compositional disorder alone. So far, studies on random systems have been focused on amorphous alloys obtained by splat cooling (Table I). To check the applicability of the theoretical models in these materials, we compute their specific-heat exponents α using the relation $\alpha = 2 - 2\beta - \gamma$. The results are listed in Table I. In fact, it is seen that within experimental uncertainties the calculated values of α are negative for the amorphous alloys studied so far. Besides these magnetization measurements, the sharpness of the Curie transition is also exhibited in the specific-heat measurements on Co-P-B and Fe-P-C alloys.[14] In crystalline elements, α was found to be positive in some cases[11] (see Table I).

2. *Magnetic equation of state*

The asymptotic form of Eq. (5) for large m, that is, when the field effect dominates over the thermal effect, is $f_\pm(m) \to m^{\delta-1}$. It can be said that Eq. (5) is another version of Eq. (3) when $m \to \infty$. However, it is not clear how much H can be increased before Eq. (3) which is supposed to be valid for small M breaks down. In the present study, it is observed that Eq. (3) is valid for fields up to 70 kOe. It might be interesting to check Eq. (3) at even higher fields. For small m, the interplay of magnetic field and thermal effects becomes important. The asymptotic forms are then obtained experimentally for materials with different magnetic properties. In $CrBr_3$, Ho and Lister[49] observed the relation $h \sim m$ for small m. Kouvel and Comly[32] obtained $h/m \sim m^2$ for nickel and CrO_2. Thus it is expected that the general asymptotic form of Eq. (5) to be given by $h/m = A_\pm + B_\pm m^2$, where the $\pm$ signs have the usual meaning. Using the definition of h and m, one can show that A_+ is given by the constant in Eq. (2), and $(A_-/B_-)^{1/2}$ is the constant in Eq. (1) which can be determined using the $M_s(T)$ and $\chi_0^{-1}(T)$ data. Other forms of Eq. (5) have been obtained[50,51] and tested experimentally[52] for all m and h using the polar parameters r and θ. Here, we do not attempt to deal with this problem in detail. Instead, we just plot m^2 vs h/m using the present data. Figure 10 shows this plot in two curves for temperatures below and above T_c. The central dash line represents the asymptotic form of the curves for large m. Thus Eq. (5) is obeyed

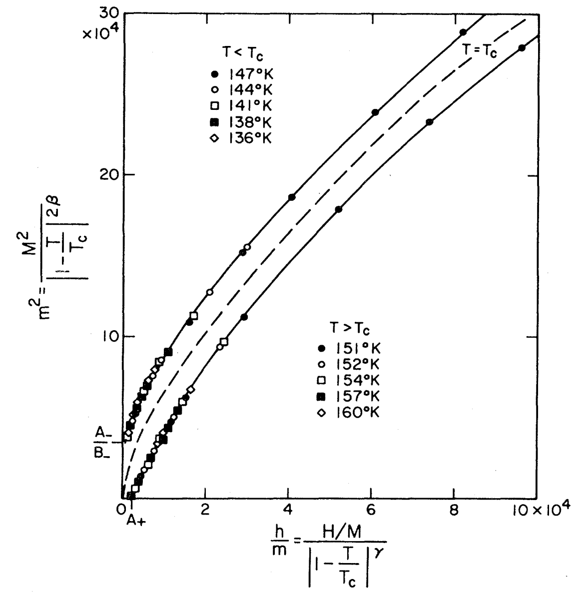

FIG. 10. Reduced magnetization m^2 vs reduced inverse susceptibility χ_0^{-1} for temperatures around T_c. The dashed line indicates asymptotic behavior of the two curves for large m above and below T_c.

over the entire range of the normalized variables.

In order to check the formerly established asymptotic relations for small m, we make a log-log plot of the small m data to verify the power law relation between m^2 and h/m. In Fig. 11, $\log_{10} m^2$ is plotted against $\log_{10}(h/m - A_+)$, where A_+ is determined from the $\chi_0^{-1}(T)$ data using Eq. (2) is found to be 1.86×10^3 Oe g/emu. Similarly, $\log_{10}(m^2 - A_-/B_-)$ vs $\log_{10}(h/m)$ is plotted in Fig. 12 with $(A_-/B_-) = 3.46 \times 10^4$ emu^2/g^2 determined from $M_s(T)$ data using Eq. (1). Two features can be realized from these plots. First, the asymptotic relations $h/m \to A_\pm + B_\pm m^2$ as $m \to 0$ are established for temperatures below and above T_c for small m. The relations for temperatures higher and lower than T_c are given by $h/m = 1.86 \times 10^3 + 0.19 m^2$ and $h/m = 0.164 m^2 - 0.566 \times 10^4$, respectively. Second, for a given temperature there is a critical field above which the asymptotic relations ($m \to 0$) are no longer obeyed. The gradients become smaller, probably tending towards the asymptotic gradient for large m given by Eq. (3). The magnitude of the critical field increases with the temperature difference $|T - T_c|$, meaning higher fields are required to compensate for the thermal effects introduced by the temperature difference $|T - T_c|$ mentioned earlier. It is interesting to note that for $|T - T_c| \simeq 12$ °K, the asymptotic relations are valid up to 40 kOe.

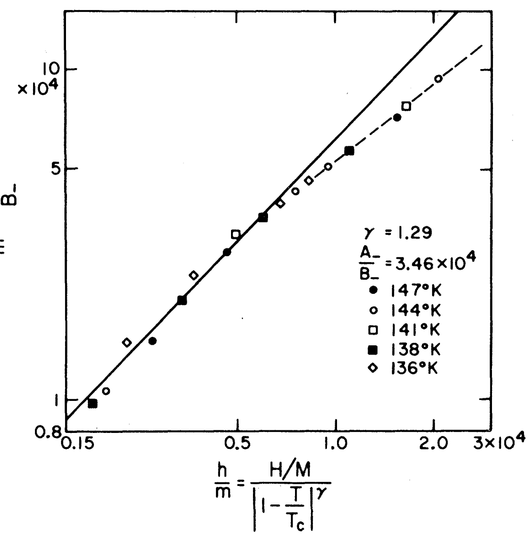

FIG. 12. $\mathrm{Log}_{10}(m^2 - A_-/B_-)$ vs $\log_{10} h/m$ determines the asymptotic equation of state for $T = T_c^-$.

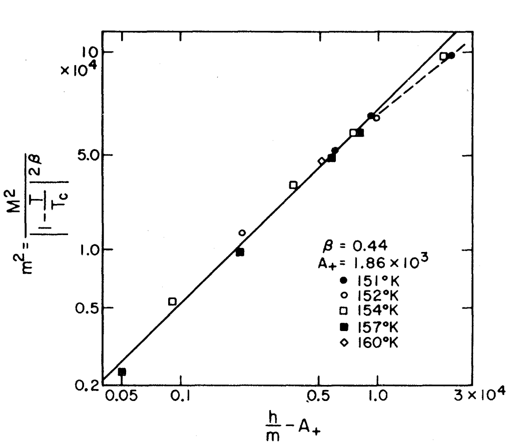

FIG. 11. $\mathrm{Log}_{10} m^2$ vs $\log_{10}(h/m - A_+)$ determines the asymptotic equation of state for $T = T_c^+$.

C. Effects of structural disorder on the magnetic properties of amorphous $Gd_{80}Au_{20}$ alloy

1. Determination of magnetic moments

The saturation magnetization was determined by the semiempirical expression[53]

$$M(H, T) = M(\infty, T)(1 - a/H) + \chi_\infty H , \quad (6)$$

where χ_∞ is the high-field susceptibility, $M(\infty, T)$ is the saturation magnetization at T °K, and a = const. The value of χ_∞ varies between different foils of the same nominal composition. The values of $M(\infty, T)$ thus obtained are plotted as a function of $T^{3/2}$ in Fig. 13. They have an uncertainty of ±1.0 emu/g. The size of the filled-circle points approximately represents this uncertainty. Within our accuracy, it is observed that the data agree well over the temperature range $0.13 < T/T_c < 0.80$

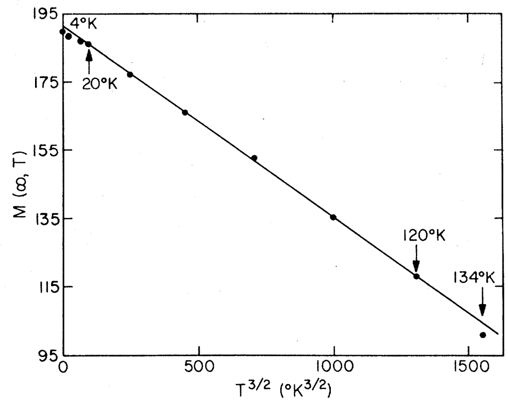

FIG. 13. Saturation magnetization $M(\infty, T)$ vs $T^{3/2}$.

with an expression of the Bloch law form

$$M(\infty, T)=M(\infty, 0)(1-bT^{3/2}), \tag{7}$$

where $M(\infty, 0)$ is the absolute saturation magnetization and $b=$ const. The departure from the straight line below 20 °K is small. Several attempts have been made to explain similar departures below 50 °K in crystalline gadolinium.[29,54]

The $Gd_{80}Au_{20}$ sample which was measured in full detail as a function of temperature in Sec. III B gives $M(\infty, 0)=192\pm1.0$ emu/g. Low-temperature magnetization measurements on three different foils of the same nominal composition exhibited some scattering (~3 percent) between the values of $M(\infty, 0)$. Thus, the value of the mean moment per atom is estimated to be $5.6\pm0.2\mu_B$. The concentration range in which the amorphous phase can be retained from splat cooling is rather small (a few percent around 20-at.% Au). From measurements on $Gd_{78}Au_{22}$ samples, it is believed that the mean moment per atom $\overline{\mu}$ varies with c (the Au content) according to the dilution law $\overline{\mu}(c)=\mu_{Gd}(1-c)$, where μ_{Gd} is the moment per atom in pure amorphous Gd. Thus, the Au atoms are unlikely to carry a substantial moment, and μ_{Gd} is estimated to be $7.0\pm0.25\mu_B$.

The agreement of the temperature dependence of the saturation magnetization for crystalline Gd with the Bloch law expression [Eq. (7)] for $0.17\leq T/T_c \leq 0.80$ was explained[55] by including the higher-order terms beyond the quadratic spin-wave dispersion in spin-wave calculations. In the case of crystalline gadolinium with a hexagonal structure, it was found that the higher-order contributions cancel each other to yield a $T^{3/2}$ behavior. However, it is not clear that the same argument holds for the amorphous $Gd_{80}Au_{20}$ alloys. The short-range order as determined from RDF on[56] $La_{80}Au_{20}$ and from analogy with equivalent amorphous systems implies that each Gd atom on the average has only eight nearest-neighboring Gd atoms and three nearest-neighboring Au atoms.

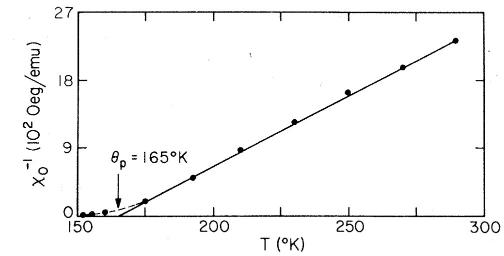

FIG. 14. Inverse susceptibility χ_0^{-1} vs temperature for $T>T_c$.

In Fig. 14, the initial susceptibility $\chi_0^{-1}(T)$ is plotted as a function of temperature. It is seen that $\chi_0^{-1}(T)$ is linear for $T>175$ °K. The paramagnetic Curie temperature θ_p is determined to be 164 ±2 °K. Assuming that the effective magnetic moment μ_{eff} is mainly due to the Gd atoms since the f shells of the Au atoms are filled, the value of μ_{eff} determined from the slope of $\chi_0^{-1}(T)$ equals 8.9 ±0.1 Bohr magnetons. This gives a total angular quantum number of $gJ=7.95\pm0.1$ using the relation $\mu_{eff}=g[J(J+1)]^{1/2}$, where g is the spectroscopic splitting factor. It is higher than the theoretical moment of $7.0\mu_B$ for the ionic $^8S_{7/2}$ state which does not include conduction-electron effects. The values of $M(\infty, 0)$, μ_{eff}, T_c, and θ_p for amorphous $Gd_{80}Au_{20}$ and crystalline Gd are listed in Table II.

In crystalline Gd, the value of saturation moment of 0 °K is enhanced by $0.5\mu_B$ over the ionic value, while the effective moment equals the ionic moment of $7\mu_B$.[57] The magnitude of the enhancement can be explained by the net spin polarization of conduction electrons.[58] In amorphous Gd-Au alloys, this enhancement effect at low temperature is not obvious. However, one must consider the possible impor-

TABLE II. Parameters derived from magnetization measurements for amorphous $Gd_{80}Au_{20}$ alloys and monocrystalline Gd.

	T_c (°K)	θ_p (°K)	μ_{eff} [a] (μ_B)	$M(\infty, 0)$ (emu/g)
Amorphous $Gd_{80}Au_{20}$	149.45 ± 0.2	164 ± 2	8.9 ± 0.1	192 ± 6
Crystalline Gd [b]	293	320	7.94	268.4

[a] $\mu_{eff}=g[J(J+1)]^{1/2}$, in μ_B per Gd atom.
[b] Reference 30, $M(\infty, 0)$ for c axis.

tance of the indirect exchange interactions among the Gd moments mediated by the Au atoms in which antiferromagnetic alignments are favored.[59] This is thought to be the case in quite a number of Gd alloys and compounds[60] where the saturation moments are found to be smaller than that in pure Gd. The enhanced μ_{eff} observed in some Gd alloys was explained by the polarization of the conduction electrons in Gd.[61] However, one should not overlook the possible presence of short-range magnetic ordering above the Curie temperature. In the case of crystalline nickel,[62] this local ordering persists up to ~$2T_c$. Indeed, the small curvatures observed in our high-field measurements (Fig. 1) at $T > T_c$ seem to support the latter argument.

2. Exchange interactions

There are two conventional methods of estimating the values of effective exchange interaction J in ferromagnets based on the Heisenberg model. One is by fitting the spin-wave theory to the experimental saturation magnetization at low temperature using the following expression[33]:

$$b = (0.0587/QS)(k_B/2JS)^{3/2}, \tag{8}$$

where b is the constant in Eq. (7), S is the ionic spin quantum number, Q equals 1, 2, 4 for simple cubic, bcc, fcc structures, respectively. A second method due to Rushbrooke and Wood[34] results from expansion of the susceptibility above the Curie temperature in powers of $J/k_B T_c$ which gives

$$k_B T_c/J = \tfrac{5}{96}(z-1)[11S(S+1)-1], \tag{9}$$

where z is the number of nearest neighbors. In crystalline gadolinium one obtains $J = 2.9$ °K from Eq. (9) knowing T_c. However, a value of 1.8 °K was obtained[40] on the basis of elementary spin-wave theory which gives Eq. (8). The discrepancy between the high- and low-temperature J values was explained by Goodings.[55] It is probably caused by the interactions beyond nearest neighbors and it was conjectured that these interactions are of the oscillatory RKKY type.[63] The magnitude of these long-range exchange interactions increases from the high-temperature molecular-field regime (χ_0^{-1} linear in T) to the low-temperature spin-wave regime.

In evaluating the values of J from Eqs. (8) and (9), we just take into account the short-range ordering in the amorphous phase. Equation (9) differs from the mean-field approximation in that the latter gives $k_B T_c/J = \frac{2}{3}zS(S+1)$. One then takes the total coordination number and uses a linear variation of the mean-exchange constant on concentration of nonmagnetic impurities. Within the mean-field theory, this procedure is equivalent to taking z as the real coordination number of magnetic atoms, which gives J as the exchange constant between the magnetic atoms. However, the difference in J obtained by these two seemingly equivalent methods is rather distinct in Eq. (9). Other dependence of J on concentration of nonmagnetic impurities have been used.[64] But they are less justifiable. In amorphous Gd-Au alloys, appropriate values of z and Q from RDF results are taken. From Ref. 56, we use $z = 8$, which implies $Q = 2$, equivalent to the bcc values. Taking $T_c = 149.45 \pm 0.2$ °K and $gS = 7.0 \pm 0.25$, the values of J obtained from Eqs. (8) and (9) are found to be 1.34 ± 0.08 and 2.28 ± 0.15 °K, respectively, which are lower than the crystalline values. Using a linear dependence of J and the total coordination number (equal to 12), one would obtain the effective exchange constants to be ~1.05 and 1.80 °K from Eqs. (8) and (9), respectively. However, the difference in J values of ~1 °K is comparable to that in crystalline Gd.

The Eqs. (8) and (9) are applicable to both $3d$ and $4f$ elements. They allow the determination of the effective constant J without implying any assumption about the nature (direct or indirect) of the exchange. It is known[57] that in rare earths the exchange is mainly of the RKKY type, the highly localized $4f$ electrons being coupled by the mediation of the conduction electrons. According to de Gennes,[63] the paramagnetic Curie temperature θ_p is related to the s-f exchange constant J_{sf} by

$$k_B \theta_P = \frac{3\pi z^2}{4E_F} J_{sf}^2 (g-1)^2 S(S+1) \sum_{j\neq i} F(2k_F R_{ij}), \tag{10}$$

where z is the number of conduction electrons per atom, E_F is the Fermi energy, and $F(\rho) = \rho^{-4}(\rho\cos\rho - \sin\rho)$ is the RKKY function. An estimate of the summation $\sum F$ is made following Ref. 63. For the double hcp structure of the lanthamide series, it was found that $\sum F \simeq 92 \times 10^{-4}$ by including only the first-nearest neighbors. Radial-distribution function (RDF) study[56] on the analogous system $La_{80}Au_{20}$ indicated that the average distance (R_{ij}) between the first-nearest-neighboring pairs of Gd atoms is similar to that in the dhcp crystalline phase, while the number of Gd nearest neighbors equals eight. Thus, summing only over the first eight Gd neighbors, we obtain $\sum F \simeq 62 \times 10^{-4}$. Taking $\theta_p = 164$ °K, $S \simeq 4$ in the paramagnetic region, $g = 2$, and $E_F \simeq 6$ eV,[63] J_{sf} is estimated to be 0.19 eV. This value remains close to that obtained by de Gennes ($J_{sf} = 0.16$ eV) for double hcp Gd. It is also in reasonable agreement with the values obtained for dilute amorphous La-Gd-Au alloys from the approach to saturation of magnetization ($J_{sf} = 0.14$ eV) and from the concentration dependence of the superconducting transition[48] ($J_{sf} = 0.16$ eV). From the very-short electron mean free path in the amorphous structure, a most severe attenuation of the RKKY interaction would be expected.[47] The fact that the RKKY exchange constant seems to be rather well preserved in our amorphous matrix is not perfectly understood.

3. Extrapolated Curie temperature for pure amorphous Gd

We plot in Fig. 15 the Curie temperatures obtained in amorphous Gd–noble-metal systems prepared by different techniques. It is seen that the experimental data obtained from sputtered[4] Gd-Ag and[3,5] Gd-Cu alloys give the same extrapolated T_c value of 250 °K for pure amorphous Gd as that obtained from the splat-cooled La-Gd-Au alloys.[65] Using the Rushbrooke-Wood formula in Eq. (9), assuming the same Gd coordination number in the amorphous state as in the crystalline state and taking the mean exchange constant $J = 2.28 \pm 0.15$ °K, T_c for pure amorphous gadolinium is estimated to be 236 ± 16 °K. The small discrepancy between the experimentally extrapolated Curie temperature and the calculated value might result from a small change in the distribution of exchange constants[21] due to alloying, thus giving a slightly different value of $\langle J \rangle$. The effect of J fluctuation on T_c is rather small for $z = 12$ and $S = \frac{7}{2}$ as predicted by the same model.

4. Fluctuations in the exchange constant

In Fig. 16, we plot the reduced spontaneous magnetization for both crystalline Gd and amorphous $Gd_{80}Au_{20}$ as a function of the reduced temperature. It can be seen that the magnetization data of $Gd_{80}Au_{20}$ lie appreciably below those of crystalline Gd. Similar behavior is observed in amorphous Fe-P-C alloys.[66] As pointed out in the latter study,

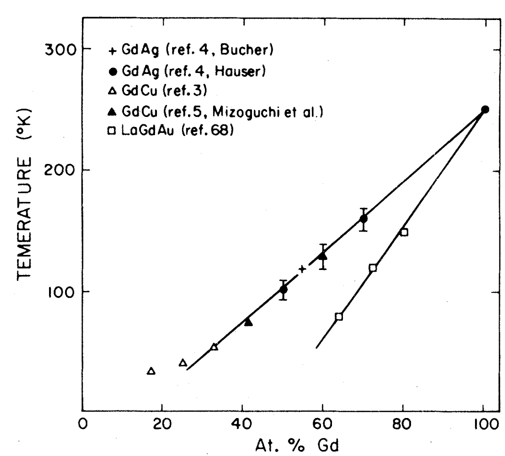

FIG. 15. Curie temperature of amorphous Gd alloys vs Gd composition. Straight lines give extrapolated Curie temperature of amorphous Gd.

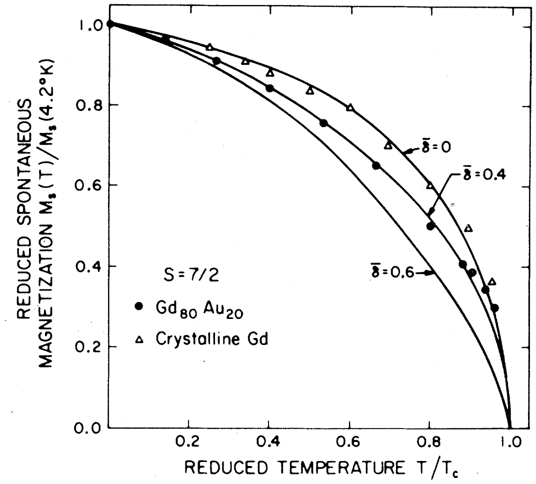

FIG. 16. Reduced spontaneous magnetization vs reduced temperature for amorphous $Gd_{80}Au_{20}$ and crystalline Gd. The Handrich theory curves for $S = \frac{7}{2}$ are plotted for mean-square fluctuations in exchange constant $\bar{\delta} = 0$, 0.4, and 0.6.

it is rather difficult to separate the effects of compositional disorder and structural disorder on the magnetization of an amorphous ferromagnet. However, from magnetization studies on amorphous Fe-P-C alloys, it is concluded that the flattening of the experimental curve in Fig. 16 is an effect of the structural disorder. Specifically, the magnetization curve for amorphous $Fe_{75}P_{15}C_{10}$ is lower than that of crystalline Fe_3P in spite of the fact that they have similar short-range orderings. Tahir-Kheli *et al.*[25] computed the magnetization for ferromagnets randomly diluted with nonmagnetic atoms using a single-site molecular-field model. They assumed negligible interactions between the magnetic and nonmagnetic atoms which is expected to apply to the present case. Their results indicated no significant depreciation in the magnetization $M_s(T)$ for ~20% dilution. However, only rather crude comparison with this model is possible, since it was derived for spin-$\frac{1}{2}$ and 1 systems. It does not seem that the large discrepancies observed both in the amorphous $Gd_{80}Au_{20}$ ($S = \frac{7}{2}$, 20% dilution) and $Fe_{75}P_{15}C_{10}$ ($S \sim 1.0$, 25% dilution) alloys can be explained by the dilution model alone. Another explanation was suggested for the amorphous rare-earth intermetallics. A constant exchange interaction between the magnetic constituents is assumed and the amorphous nature of the alloy is manifested in a random distribution of local anisotropy field.[28,67] However, the latter approach is irrelevent to our present study of Gd-Au alloys, because of the S character of Gd ions.

We think that the structural fluctuations in our amorphous alloy are reflected by a distribution of exchange integrals.[20-22] Using Handrich's theory,[21] we evaluate the effect of structural disorder on the fluctuations in the exchange constant. Based on the molecular field approach from the Heisenberg Hamiltonian, the following equation of state for the reduced spontaneous magnetization is obtained:

$$M(T)=\tfrac{1}{2}\{B_s[(1+\bar{\delta})x]+B_s[(1-\bar{\delta})x]\}, \qquad (11)$$

where $x=[3M(T)/(S+1)]T_c/T$, and $\bar{\delta}$ is the root mean square of deviation from an average exchange constant between two nearest-neighbor spins in the presence of disorder:

$$\bar{\delta}^2=\langle\Delta J^2\rangle/\langle J\rangle^2 .$$

Magnetization curves calculated from Eq. (11) for the case of $S=\frac{7}{2}$ and various values of $\bar{\delta}$ are shown in Fig. 16. Within experimental uncertainties, it is found that the curve with $\bar{\delta}=0.4$ gives a rather good overall fit to the experimental data. As expected, the crystalline Gd data fit the $\bar{\delta}=0$ curve very well. This gives an order of estimate of the fluctuations in the exchange interaction. It suggests that the average variation in J can be an appreciable fraction of J itself. Similar magnitude of $\bar{\delta}$ was also observed in amorphous Fe-P-C alloys.[66] Our values of J evaluated beforehand from Eqs. (8) and (9) can be regarded as the average exchange constant.

In conclusion, both the Curie temperature and magnetic moment in the amorphous system can be tentatively compared with those in the crystalline counterpart. In the absence of any crystalline $Gd_{80}Au_{20}$ phase, we compare the extrapolated values in amorphous Gd to those in crystalline Gd. The Curie temperature is estimated to depreciate by $\gtrsim$15% and the saturation moment by $\lesssim$8% in the amorphous state. This disagrees with Darby's calculation[68] of the crystal-field effects on the magnetic properties of amorphous Gd. To compare with amorphous transition-metal alloys: in $Fe_{75}P_6B_{19}$,[69] the respective depreciations are 12% for T_c and 7% for μ; smaller depreciations are observed in Fe-P-C and Co-Si-B systems.[70] The effect of amorphousness on the bulk magnetic properties as well as on the distribution in exchange integrals is thus about the same in magnitude for amorphous Gd alloys with high Gd content as for $3d$-based amorphous alloys.

IV. SUMMARY AND CONCLUSION

Our detail analysis of the magnetization data in the vicinity of the Curie transition in amorphous $Gd_{80}Au_{20}$ alloys allow us to give reliable values for the critical exponents. Some points have to be emphasized. First, due to the magnetic contribution from crystalline precipitates, (a few percent of the sample), the low-field data around T_c have to be handled with extreme care. Already present in rather homogeneous splat-cooled amorphous alloys, this difficulty might be overwhelming in other preparation techniques. Second, the trend of enhanced values for the magnetization exponent β has to be checked in various disordered and amorphous systems. Third, specific-heat measurements around T_c are needed for a meaningful comparison of the experimental results with recent theories on magnetic phase transition in amorphous materials.

The effect of amorphousness on the magnetic properties of $Gd_{80}Au_{20}$ alloys seems to be reflected mainly by a distribution of the exchange integrals in the Heisenberg model. So far as the mean values are concerned, the structural disorder results in a a slight reduction in the magnetic parameters (e.g., μ_{Gd}, μ_{eff}, J_{sf}, and $\langle J\rangle\cdots$ as defined in text). From the weak magnetic anisotropy and the absence of crystal-field effects in Gd, our amorphous alloys with high Gd content represent a simple case where the RKKY interactions are evidenced as a predominant coupling mechanism. The most intriguing result might be that these long-range RKKY interactions seem to be essentially preserved in spite of the drastic reduction in the electronic mean free path. This preliminary conclusion calls for further experimental and theoretical investigations.

Note added in proof. From recent specific-heat measurements, the exponent α was determined for pure crystalline Gd ($\alpha=-0.20\pm0.02$) [M. B. Salamon, D. S. Simmons, and C. C. Huang, Physica 86–88B, 583 (1977)] and for amorphous $Fe_{75}P_{15}C_{10}$ ($\alpha=-0.21\pm0.02$) [L. J. Schowalter, M. B. Salamon, C. C. Tsuei, and R. A. Craven, Bull. Am. Phys. Soc. 22, 264 (1977)].

ACKNOWLEDGMENT

The authors wish to thank Professor P. Duwez for his interest and support throughout this work.

*Work supported by the ERDA, Contract No. AT(04-3)-822.

†On leave from Laboratoire de Structure Electronique des Solides, E. R. A. 100, rue Blaise Pascal, 67000 Strasbourg, France.

[1] K. Lee and N. Heiman, AIP Conf. Proc. 24, 108 (1975).

[2] H. A. Alperin, J. R. Cullen, and A. E. Clark, AIP Conf. Proc. 29. 186 (1976).

[3] N. Heiman and K. Lee, AIP Conf. Proc. 34, 319 (1976).

[4] S. W. Charles, J. Popplewell, and P. A. Bates, J. Phys. F 3, 664 (1973); B. Boucher, J. Phys. (Paris) 37, L-345 (1976); J. J. Hauser, Phys. Rev. B 12, 5160 (1975).

[5] T. R. McGuire, R. C. Taylor, and R. J. Gambino, AIP

Conf. Proc. 34, 346 (1976); T. Mizoguchi, T. R. McGuire, S. Kirkpatrick, and R. J. Gambino, Physica 86–88B, 783 (1977).

[6]W. L. Johnson, S. J. Poon, and P. Duwez, Phys. Rev. B 11, 150 (1975).

[7]N. Heiman, K. Lee, and R. I. Potter, AIP Conf. Proc. 29, 130 (1976).

[8]N. Heiman, K. Lee, R. I. Potter, and S. Kirkpatrick, J. Appl. Phys. 47, 2634 (1976).

[9]J. J. Rhyne, S. J. Pickart, and H. A. Alperin, AIP Conf. Proc. 18, 563 (1974); J. M. D. Coey, J. Chappert, J. P. Rebouillat, and T. S. Wang, Phys. Rev. Lett. 36, 1061 (1976); R. Arrese-Boggiano, J. Chappert, J. M. D. Coey, A. Lienard, and J. P. Rebouillat, J. Phys. (Paris) 37, C6-771 (1977); J. P. Rebouillat, A. Lienard, J. M. D. Coey, R. Arrese-Boggiano, and J. Chappert, Physica 86–88B, 773 (1977).

[10]M. E. Fisher, Phys. Rev. 176, 257 (1968); A. Brooks Harris, J. Phys. C 7, 1671 (1974), and references cited therein.

[11]A. Brooks Harris and T. C. Lubensky, Phys. Rev. Lett. 33, 1540 (1974); T. C. Lubensky and A. B. Harris, AIP Conf. Proc. 24, 311 (1975).

[12]U. Krey, Phys. Lett. A 51, 189 (1975); G. Grinstein and A. Luther, Phys. Rev. B 13, 1329 (1976).

[13]H. Müller-Krumbhaar, J. Phys. C 9, 345 (1976), and references cited therein.

[14]T. Mizoguchi and K. Yamauchi, J. Phys. (Paris) 35, C4-287 (1974); T. Mizoguchi, AIP Conf. Proc. 34, 286 (1976); K. Yamada, Y. Ishikawa, Y. Endoh, and T. Masumoto, Solid State Commun. 16, 1335 (1975); E. Figueroa, L. Lundgren, O. Beckman, and S. M. Bhagat, *ibid.* 20, 961 (1976).

[15]See, for example, H. E. Stanley, in *Introduction to Phase Transitions Critical Phenomena* (Oxford University, New York, 1971); M. Vicentini-Missoni, J. M. H. Levelt Sengers, and M. S. Green, J. Res. Natl. Bur. Std. (U.S.) A 73, 563 (1969). For more recent reviews, see, M. E. Fisher, Rev. Mod. Phys. 46, 597 (1974); L. P. Kadanoff, in *Phase Transition and Critical Phenomena,* edited by C. Domb and M. S. Green (Academic, New York, 1976), Vol. 5A, p. 18.

[16]J. S. Kouvel and D. S. Rodbell, Phys. Rev. Lett. 18, 215 (1967).

[17]A. Arrott and J. E. Noakes, Phys. Rev. Lett. 19, 786 (1967), and references cited therein.

[18]J. S. Kouvel and M. E. Fisher, Phys. Rev. 136, A1626 (1964).

[19]M. N. Deschizeaux and G. Develey, J. Phys. (Paris) 32, 319 (1971).

[20]A. I. Gubanov, Fiz. Taverd. Tela 2, 502 (1960) [Sov. Phys.-Solid State 2, 468 (1961)].

[21]K. Handrich, Phys. Status Solidi 32, K55 (1969); Phys. Status Solidi B 53, K17 (1972). J. Schreiber, S. Kobe, K. Handrich, and J. Richter, *ibid.* 70, 673 (1975).

[22]T. Kaneyoshi, J. Phys. C 6, L19 (1973).

[23]R. A. Tahir-Kheli, Phys. Rev. B 6, 2808 (1972); in *Amorphous Magnetism*, edited by H. O. Hooper and de Graaf (Plenum, New York, 1973), p. 393; Solid State Commun. 19, 1213 (1976), and references cited therein.

[24]R. A. Tahir-Kheli, L. C. M. Miranda, and S. M. Rezende, AIP Conf. Proc. 18, 610 (1974).

[25]R. A. Tahir-Kheli and L. C. M. Miranda, Nuovo Cimento B 30, 335 (1975), and references cited therein.

[26]A. B. Harris, P. L. Leath, B. G. Nickel, and R. J. Elliott, J. Phys. C 7, 1693 (1974).

[27]J. Schreiber, Phys. Status Solidi B 59, K119 (1973).

[28]R. Harris, M. Plischke, and M. J. Zuckermann, Phys. Rev. Lett. 31, 160 (1973); J. Phys. (Paris) 35, C4–265 (1974).

[29]See, for example, T. Kasuya, in *Magnetism*, edited by G. T. Rado and H. Suhl (Academic, New York, 1966), Vol. IIB, p. 215.

[30]H. E. Nigh, S. Legvold, and F. H. Spedding, Phys. Rev. 132, 1092 (1963).

[31]C. D. Graham, Jr., J. Appl. Phys. 36, 1135 (1965).

[32]J. S. Kouvel and J. B. Comly, Phys. Rev. Lett. 20, 1237 (1968).

[33]J. A. Hoffmann, A. Paskin, K. J. Taner, and R. J. Weiss, J. Phys. Chem. Solids 1, 45 (1956); 15, 187 (1960).

[34]G. S. Rushbrooke and P. J. Wood, Mol. Phys. 1, 258 (1958).

[35]P. Duwez, in *Progress in Solid State Chemistry* (Pergamon, Oxford, 1966), Vol. 3, p. 377.

[36]W. L. Johnson and S. J. Poon, J. Appl. Phys. 46, 1787 (1975).

[37]G. Tangonan, Ph.D. thesis (Caltech, 1975) (unpublished).

[38]A. Amamou, IEEE Trans. Magn. 12, 948 (1976).

[39]A. Amamou and J. Durand, Commun. Phys. 1, 191 (1976).

[40]J. F. Elliott, S. Legvold, and F. H. Spedding, Phys. Rev. 91, 28 (1953).

[41]C. Domb and D. L. Hunter, Proc. Phys. Soc. Lond. 86, 1147 (1965).

[42]B. Widom, J. Chem. Phys. 43, 3898 (1965).

[43]L. P. Kadanoff, Physics 2, 263 (1966).

[44]A. Arrott, Phys. Rev. 108, 1394 (1957).

[45]J. S. Kouvel, General Electrics Res. Lab. Rep. No. 57–RL–1799 (1957) (unpublished).

[46]L. P. Kadanoff *et al.*, Rev. Mod. Phys. 39, 395 (1967).

[47]P. G. de Gennes, J. Phys. Radium 23, 630 (1962); T. Kaneyoshi, J. Phys. F 5, 1014 (1975).

[48]S. J. Poon and J. Durand, Solid State Commun. 21, 793 (1977); and 21, 999 (1977); 22, 475 (1977); Commun. Phys. (to be published).

[49]J. T. Ho and J. D. Lister, Phys. Rev. Lett. 22, 603 (1969).

[50]P. Schofield, Phys. Rev. Lett. 22, 606 (1969).

[51]B. D. Josephson, J. Phys. C 2, 1113 (1969).

[52]J. T. Ho, Phys. Rev. Lett. 26, 1485 (1971).

[53]A. Herpin, in *Théorie Du Magnêtisme* (Universitaires de France, Paris, 1968), p. 831.

[54]W. N. R. Stevens, J. Phys. C 2, 339 (1969).

[55]D. A. Goodings, Phys. Rev. 127, 1532 (1962).

[56]J. Logan, Scr. Metall. 9, 379 (1975); G. S. Cargill III, in *Solid State Physics*, edited by Seitz *et al*. (Academic, New York, 1975), Vol. 30, p. 225.

[57]See, for example, J. J. Rhyne, in *Magnetic Properties of Rare Earth Metals*, edited by R. J. Elliott (Plenum, London, 1972), p. 129; also A. J. Freeman, *ibid.* p. 245.

[58]J. Geldenhuys and D. H. Wiid, Solid State Commun. 20, 337 (1976).

[59]F. Kissel and W. E. Wallace, J. Less-Common Met.

11, 417 (1966).
[60]K. H. J. Buschow and C. J. Schinkel, Solid State Commun. 18, 609 (1976), and references cited therein.
[61]W. C. Thoburn, S. Legvold, and F. H. Spedding, Phys. Rev. 110, 1298 (1958).
[62]P. A. Beck and C. P. Flynn, Solid State Commun. 18, 127 (1976).
[63]P. G. de Gennes, J. Phys. Radium 23, 510 (1962).
[64]See, for example, A. B. Beznosov and V. G. Nazarenko, Fiz. Tverd. Tela 16, 576 (1974) [Sov. Phys.-Solid State 16, 372 (1974)].
[65]S.J. Poon and J. Durand, in Amorphous Magnetism II, edited by R. A. Levy and R. Hasegawa (Plenum, New York, to be published).
[66]C. C. Tsuei and H. Lilienthal, Phys. Rev. B 13, 4899 (1976).
[67]J. E. Gubernatis and P. L. Taylor, Phys. Lett. A 43, 211 (1973).
[68]M. I. Darby, J. Non-Cryst. Solids 20, 357 (1976).
[69]J. Durand, IEEE Trans. Magn. 12, 945 (1976).
[70]H. Kazama, M. Kameda, and T. Masumoto, AIP Conf. Proc. 34, 307 (1976).